Shock interaction at Mach 4 of a water and fuel droplet

VIROT F.[1], RULLIER J-L.[2], HEBERT D. [2]

[1] *PPrime Institute, CNRS, ISAE-ENSMA, Université de Poitiers*
1 avenue Clément Ader, BP40109
86961Futuroscope Chassneuil Cedex, France

[2] *CEA DAM, CESTA, 15 Avenue des Sablières CS60001,*
33116 Le Barp Cedex, France

1 Introduction

Shock droplet interactions study actually starts from the 60's for the needs of propulsion developments in rocket or diesel combustion engines as reminded in Kailasanath's review [1] and is still attractive nowadays for future pressure gain combustion systems such as the rotating detonation engine (RDE). Indeed, the latter is a candidate for next generation of propulsion systems that would be more efficient and could reduce environmental impact in transportation. The use of liquid fuel is also of considerable interest in reducing the volume and weight for aero-propulsive vehicles.

Numerous works have been done to understand the physical mechanisms of the shock wave interaction with the droplet, that is inert or fuel, then the mixing of the vapour phase with the oxidizer for combustion and heat release. Guildenbecher et al. wrote a review about them [2]. Nethertheless very few experiments are reported for high shock Mach number M_s when conditions approach those of a detonation. Reinecke and McKay [3] or Pinaev and Sychev [4] are among the exceptions.

Small fuel droplet sizes < 10 µm and/or high pressure vapor fuels are considered to have behavior similar to gas. On the contrary, large droplets and low vapor pressure fuel are much difficult to detonate. For instance, no detonation was successful when mean droplet sizes of decane/air or dodecane/air are larger than 30 µm in Mar's experiments [5].

With the experimental device used in previous work [6], the image sequences of the drop disintegration for long time are conducted for a M_s=4 shock wave propagating in air at initial atmospheric pressure and impacting an isolated droplet of water or n-dodecane. Besides, high resolution images is useful for CFD codes validation [7].

2 Experimental setup

The experimental device used in this work is shown in Figure 1 : it is composed by a round 92 mm inner diameter detonation tube with a booster section, a detonation driver section, a test section filled with air and ended by a vacuumed dump tank. Each section is separated by a 100 µm plastic diaphragm (Mylar) that allows specific gas composition and initial pressure. A detonation is successively generated in the 1 m-long booster section filled with a stoichiometric H_2/O_2 mixture thanks to an electric igniter, then in the 7 m-long detonation driver part filled with a less detonation sensitive H_2+0.5 O_2+3.33 He mixture. As the detonation propagates to the right and consumes all the reactive mixture, the latter interacts with the air of the test section by producing a strong shock wave. The shock wave forms and stabilizes in a 1.48 m long section before entering a 0.12 m-long round-to-square transition section adjacent to the 80 mm x 80 mm square section chamber in which a water droplet is suspended on two tiny crossed copper wires, having a negligible size (diameter 25 µm) compared to the droplet diameter. Pressure signals are recorded by Kistler 603B sensors (with their Kistler 5011 charge amplifiers) on a National Instrument PXI-5105 digitizer at 60 Mhz. These allow to monitor detonation and shock velocities and to trig the camera.

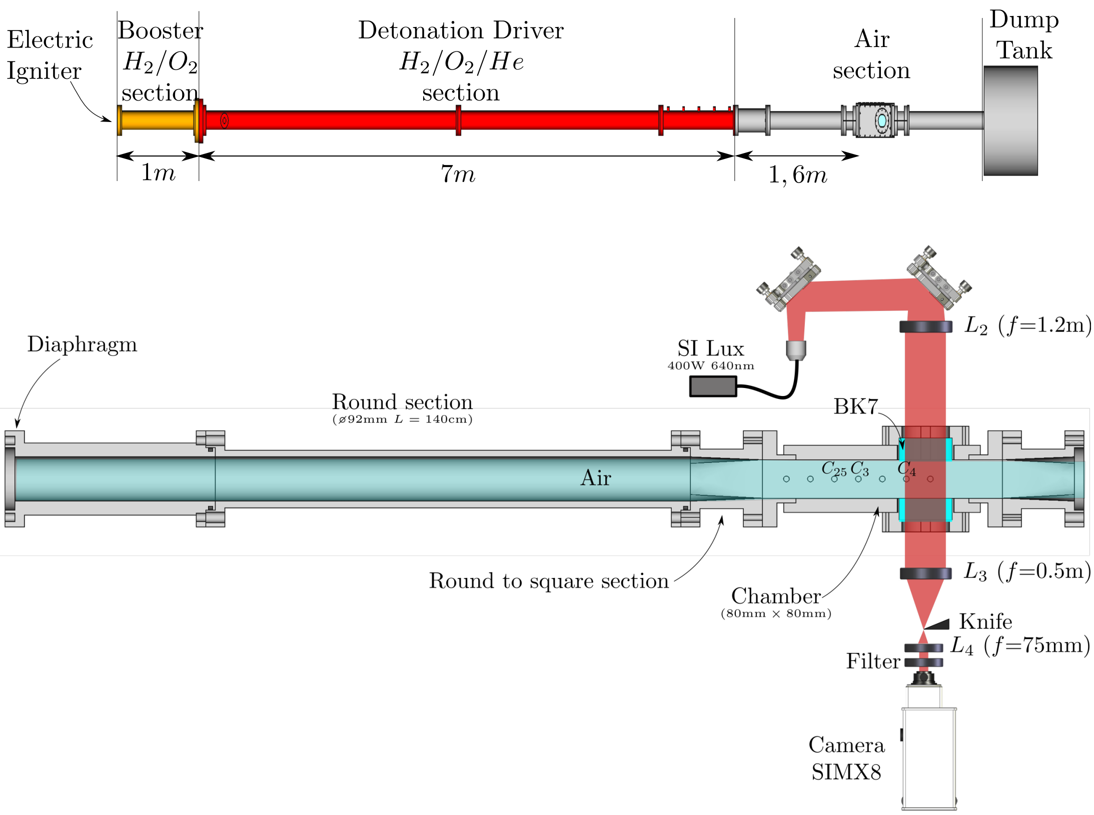

Figure 1 Sketch of the experimental detonation tube to generate Mach 4 shock waves (top) and the optical configuration (bottom)

The interactions occurring between the shock wave and the water droplet are recorded using schlieren technique with a pulsed monochromatic light source red (SI-Lux, 400 W, 640 nm) through two BK7 optical ports (oblong windows 90 mm x 70 mm). An ultra-high-speed camera Specialized Imaging SIM records 8 images with 20 ns exposure time and 5-10 µs interframe delay. Sensor resolution of 1360 x 1024 pixels leads to a resolution of 23 pxl/mm.

3 Results with a water droplet

Experiments are conducted at ambient conditions (atmospheric pressure and 20°C) for air in the test section. Initial pressures of booster and driver sections are adjusted in order to generate a shock wave at Mach 4.3±0.2 and the droplet diameter is varied between 430 µm and 850 µm. For air initially at rest at P_0=101.325 kPa and T_0=293 K, the Mach 4 shock wave travels at 1375 m/s. Pressure, temperature, density and gas particle velocity behind the front are 1.94 MPa, 1140 K, 5.9 kg/m^3 and 1094 m/s respectively.

Figure 2 shows an example of a test with a medium size droplet of diameter D=630 µm. Absolute

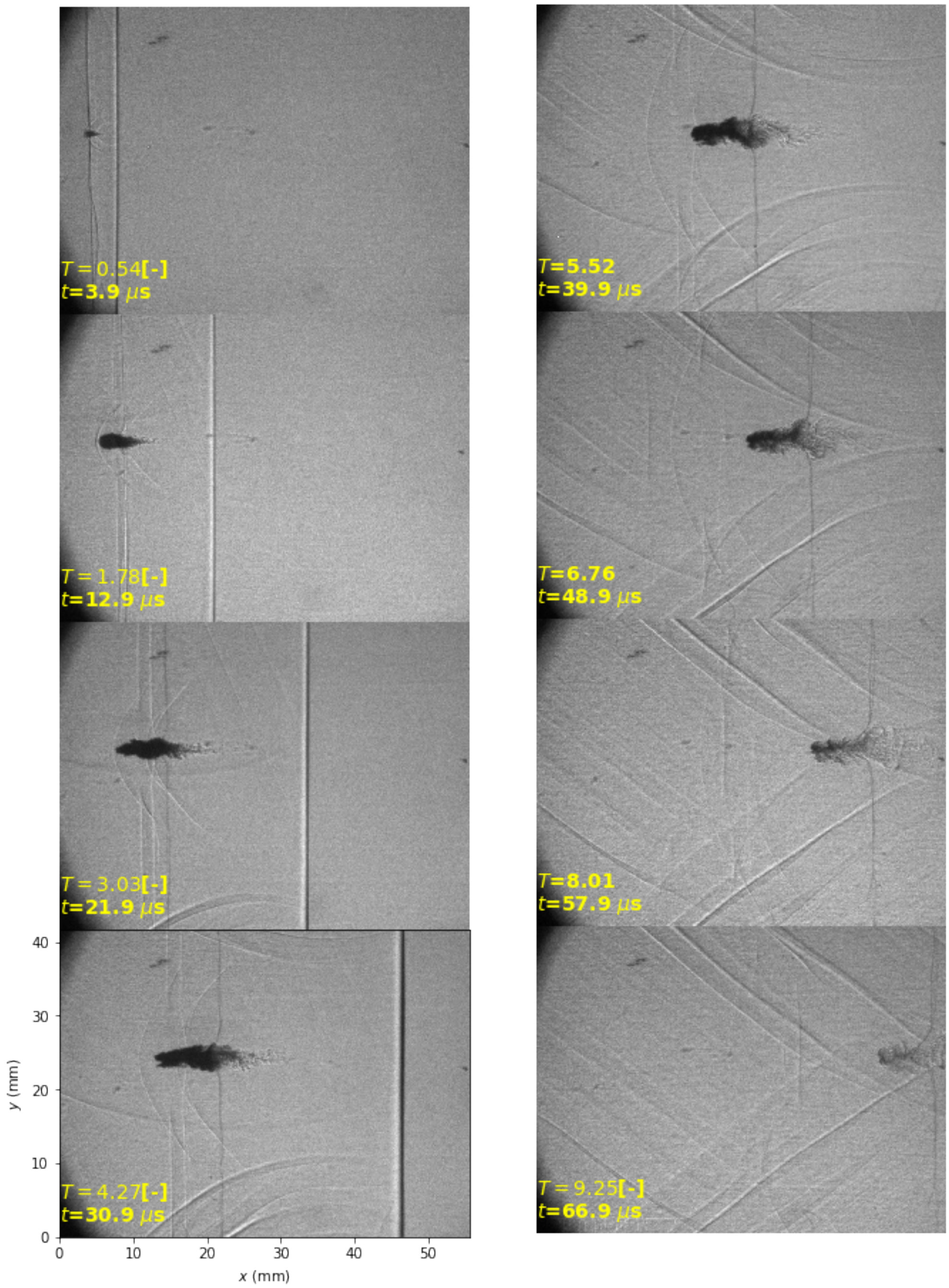

Figure 2 Images of a Mach 4.1 shock wave impacting a D=630 µm water droplet (We≈66000).

time from the shock impacting the droplet t along with dimensionless time $T = \frac{t}{t_r}$ are added on each frame where $t_r = \frac{D}{u_1}\sqrt{\frac{\rho_1}{\rho_l}}$ stands for the Rayleigh time with ρ_1, u_1 the post shock density and absolute velocity of gas respectively, and ρ_l the droplet density.

Shock passage over the droplet induces its deformation in early times which takes a disk shape of 3 initial drop diameter D when $T \approx 1.5$ as already shown by Pilch and Erdmann [7]. The flow around the drop leads small droplets in the tail which make an opaque mist that follows the droplet. In previous experiments [6], the window size does not allow to visualize after $T > 5$; thus diminution of opacity of the mist was not observable. In the last frame of Figure 2, few mist remains.

Figure 3 presents the evolution of the drop position x_d along with its dimensionless position $X_d = \frac{x\_d}{D}$. As expected, and in extension to previous study [6], physical position and time give sparse data contrary

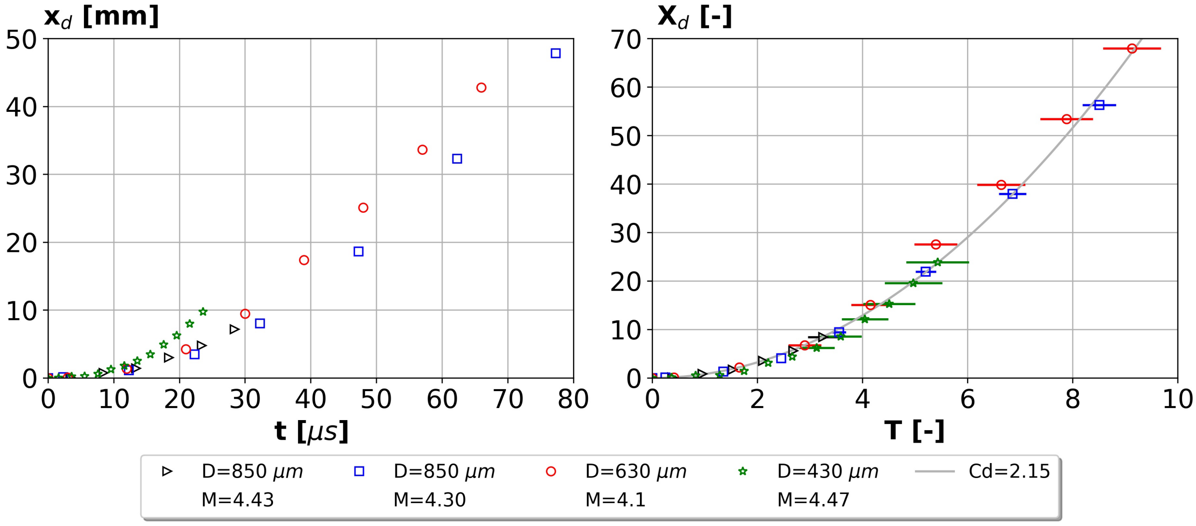

Figure 3 Evolution of the water droplet position in function of time (left: physical time and position; right dimensionless time and position)

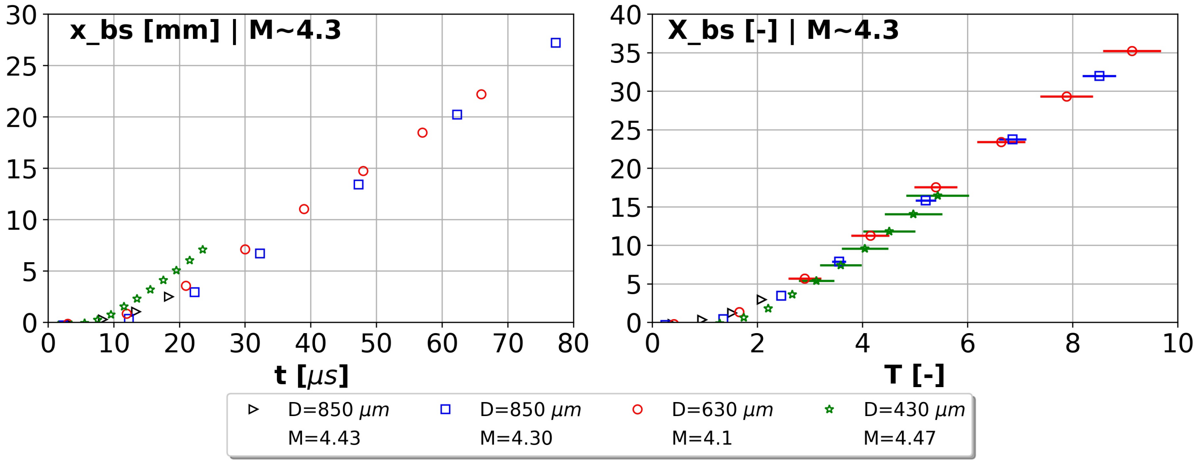

Figure 4 Evolution of bow shock distance to the water droplet in function of time (left: physical time and distance; right dimensionless time and distance)

to the X_d, T space where X_d follows a second order law in T up to $T \approx 9$. Similarly with the equation of motion of a rigid sphere $X = \frac{3}{8} C_D T^2$, a drag coefficient $C_D = 2.15$ is obtained as parameter result of the fitting.

Figure 4 plots the evolution of the position of the bow shock in front of the drop (i.e its most left position), both in physical and dimensionless spaces. Sparse data in physical space merges into a well grouped curve as same manner as for X_d and, for $T > 3$, a linear law can be extracted from data giving $X_{bs} = 5(T - 2)$.

4 Preliminary results for a n-Dodecane droplet

Tests have been conducted in the detonation driven shock tube with a drop of n-Decane which is known as very low volatile fuel. This result is obtained with an exposure time of 240 ns and 14.3 µs interframe delay to catch different behavior compared to water droplet and possible ignition of daughter droplets. An example is given in Figure 5 where no ignition was detected up to $T = 4.65$. Next experiments will be done with longer T and a detailed comparison with a water droplet will be addressed.

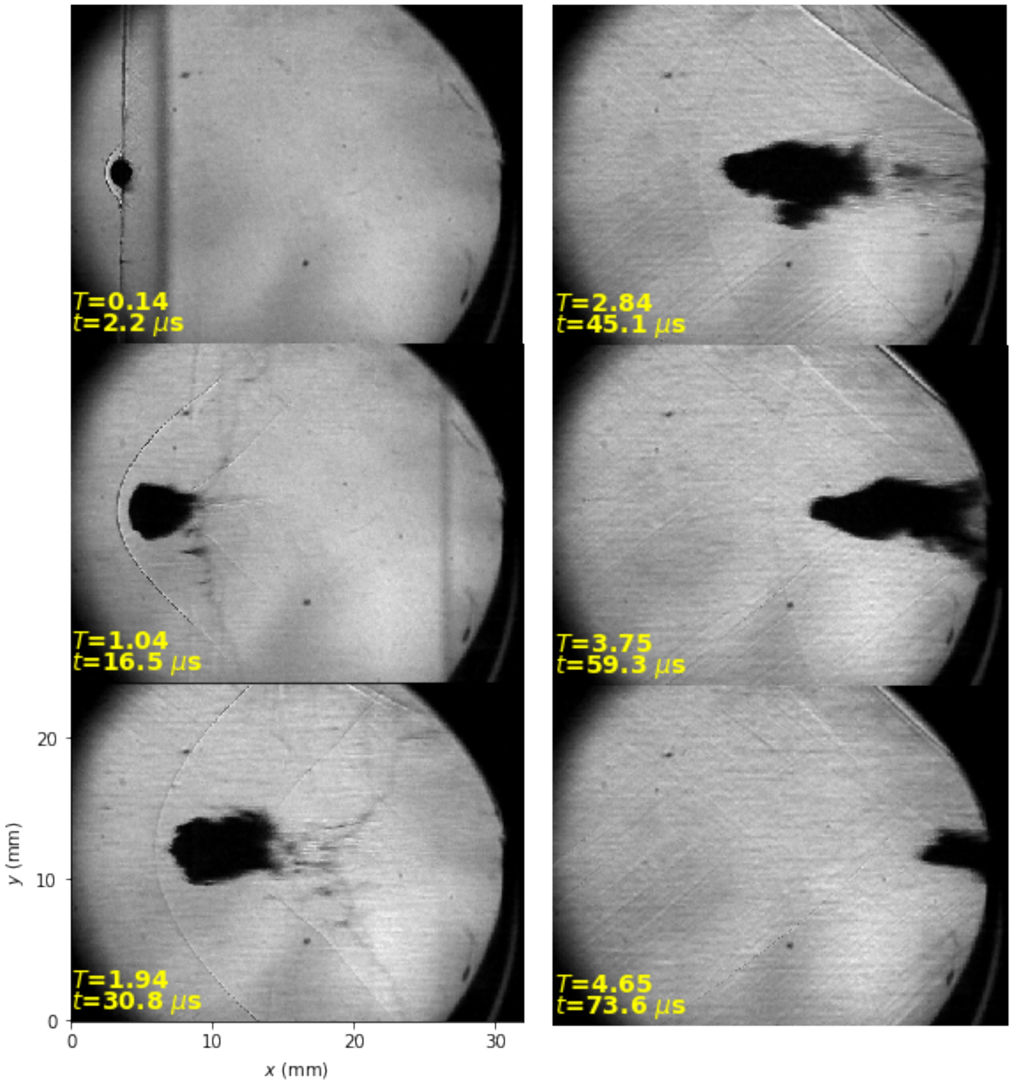

Figure 5 Shock wave impacting a 1.6 mm n-dodecane droplet at Mach 4.

5 Conclusion

Experiments on the interaction between a drop and a shock wave at around Mach 4 in air were carried out using a detonation driven shock tube. Special cares have been taken in order to obtain a sequence of high resolution frames.

Evolution of water droplets of diameter from 430 μm to 850 μm has been recorded up to $T \approx 9$. Analysis of droplet positions agrees with a second order law for dimensionless space X_d, T and a drag coefficient $C_D = 2.15$ associated to the fitting was verified and extended to these long T. As the same manner, positions of the bow shock in front of the droplet follow a tendency in dimensionless space with a linear evolution when $T > 3$.

Experiments with n-dodecane demonstrate feasibility to test a low vapor pressure fuel with our previous setup and a comparison with water droplet will be addressed.

References

[1] K. Kailasanath, "Liquid-Fueled Detonations in Tubes," *Journal of Propulsion and Power,* vol. 22, no. 6, pp. 1261-1268, 2006.

[2] D. Guildenbecher, C. Lopez-Rivera and P. Sojka, "Secondary atomization," *Experiment in fliuds,* vol. 46, pp. 371-402, 2009.

[3] W. Reinecke and W. McKay, "Experiments on water drop breakup behind Mach 3 to 12 shocks," Tech. rep. SC-CR-70-6063, Avco Government Products Group, 1969.

[4] A. Pinaev and A. Sychev, "Ignition of fuel droplets behind a shock wave front," *Combustion, Explosion and Shock Waves,* vol. 18, no. 6, pp. 81-90, 1982.

[5] M. Mar, "Détonations dans les aérosols de gouttelettes de carburants liquides: étude de l'influence de la granulométrie des gouttelettes," PhD ISAE-ENSMA, Poitiers, 2012.

[6] D. Hébert, J.-L. Rullier, J.-M. Chevalier, I. Bertron, E. Lescoute, F. Virot and H. El-Rabii, "Investigation of mechanisms leading to water drop breakup at Mach 4.4 and Weber numbers above 10^5," *SN Applied Sciences,* vol. 2, no. 69, pp. 1-20, 2020.

[7] G. Tymen, D. Hébert, J.-L. Rullier, T. Bridel-Bertomeu, I. Berton, S. Peluchon, E. Lescoute and F. Virot, "Numerical investigation of the interactions between a low-hypersonic shock wave and a water droplet : VOF and DI methods comparison," *International Journal of Computational Methods and Experimental Measurements,* vol. 11, pp. 341-354, 2020.

[8] M. Pilch and C. Erdman, "Use of breakup time data and velocity history data to predict the maximum size of stable fragments for acceleration-induced breakup of a liquid drop," *International Journal of Multiphase Flow,* vol. 13, no. 6, pp. 741 - 757, 1987.